13th IFAC Symposium on Control in Transportation Systems
The International Federation of Automatic Control
September 12-14, 2012. Sofia, Bulgaria

Integrated Ramp Metering and Mainstream Traffic Flow Control on Freeways Using Variable Speed Limits

Rodrigo C. Carlson*. Diamantis Manolis***
Ioannis Papamichail*. Markos Papageorgiou*

*Technical University of Crete, Chania, 73100, Greece
(Fax: +30 28210-37584; e-mails:<rcarlson;dmanolis;ipapa;markos>@dssl.tuc.gr).
**The Capes Foundation, Ministry of Education of Brazil

Abstract: In this paper we integrate local ramp metering (RM) with Mainstream Traffic Flow Control (MTFC) enabled via Variable Speed Limits (VSL), which is a recently proposed freeway traffic management tool. The integration is performed by the extension of an existing simple local cascade feedback MTFC controller via a split-range-like scheme. The integrated controller remains simple yet efficient and suitable for field implementation. The controller is evaluated in simulation and compared to stand-alone RM or MTFC via VSL, as well as optimal control results. The controller's performance is shown to meet the specifications and to approach the optimal control results for the investigated scenario.

Keywords: feedback control, split-range control, integrated traffic control, freeway traffic flow control, mainstream traffic flow control, ramp metering, variable speed limits.

1. INTRODUCTION

Traffic flow congestion on freeways is an increasing problem of modern societies with serious impact on travel times, traffic safety, fuel consumption and environmental pollution. Various traffic control measures have been proposed to alleviate traffic congestion but are known to face limitations. Ramp Metering (RM), for example, is the most direct and efficient tool for freeway traffic flow control but because the ramp storage space may be limited, RM may have to be deactivated for most of the peak period due to full ramps (Papamichail et al., 2010). To overcome these limitations, the integration of traffic control measures has been investigated in the past, for example RM integrated with route guidance (Kotsialos et al., 2002; Karimi et al., 2004); or RM integrated with variable speed limits (VSL) (Hegyi et al., 2005; Zhang et al., 2006). Most of these approaches were, however, based on methods that may face difficulties in field applications; in some cases even simulation results were not satisfactory.

Recently, Carlson et al. (2010a, 2010b) proposed Mainstream Traffic Flow Control (MTFC) on freeways by the use of VSL and investigated its integration with RM via an optimal control approach. Because of the limited practicality of the optimal control approach employed, Carlson et al. (2011) designed a simple but efficient feedback MTFC controller without considering, however, the integration with RM.

We propose the integration of MTFC via VSL with RM using a feedback control approach. The feedback MTFC controller developed by Carlson et al. (2011) is extended via a split-range-like scheme (Stephanopoulos, 1984). Simulation-based investigations for a hypothetical freeway network using the METANET simulator (Messmer and Papageorgiou, 1990) demonstrate the features of the proposed integrated control strategy and compare its efficiency against stand-alone RM, MTFC via VSL and an optimal control approach.

In Section 2, the congestion-caused infrastructure degradation and the MTFC concept are reviewed, along with an outline of the METANET simulator and the AMOC optimal control tool (Kotsialos et al., 2002) used for the evaluation of the proposed strategy. Section 3 presents the feedback control strategies employed in this paper and the design of the integrated controller. Their efficiency is evaluated in Section 4. Finally, Section 5 concludes the paper.

2. BACKGROUND

2.1 Congestion-caused Infrastructure Degradation and the MTFC Concept

A (latent) bottleneck on a freeway is a location where the flow capacity $q_{\mathrm{cap}}^{\mathrm{up}}$ upstream is higher than the flow capacity $q_{\mathrm{cap}}^{\mathrm{down}}$ downstream of the bottleneck location (Fig. 1). If the arriving flow q_{in} (which verifies $q_{\mathrm{in}} \le q_{\mathrm{cap}}^{\mathrm{up}}$) is higher than $q_{\mathrm{cap}}^{\mathrm{down}}$, the bottleneck is activated, i.e., a congestion is formed (Fig. 1). The congestion forming at an active bottleneck has two kinds of detrimental effects on the freeway capacity and throughput (Papageorgiou and Kotsialos, 2002):

- *Capacity drop (CD)* at the congestion head, i.e., an active bottleneck outflow q_{out} that may be 5-20% lower than the nominal capacity $q_{\mathrm{cap}}^{\mathrm{down}}$. A main contributing factor for CD is deemed to be the acceleration of vehicles while exiting the congested area.
- *Blocking of off-ramps (BOR)*: vehicles that are bound for exits upstream of the active bottleneck are delayed due to the blocking of off-ramps by the congestion body, whereby off-ramp flow is reduced.

MTFC regulates the mainstream traffic flow sufficiently

978-3-902823-13-7/12/$20.00 © 2012 IFAC
10.3182/20120912-3-BG-2031.00021

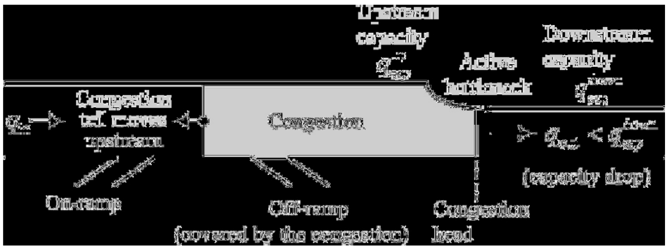

Fig. 1. Active bottleneck notions.

upstream of (otherwise) active bottlenecks so as to avoid the CD (since vehicles will have accelerated before reaching the bottleneck area). The bottleneck of Fig. 2 is not activated (and no MTFC is needed) as long as $q_{\text{in}} \le q_{\text{cap}}^{\text{down}}$, in which case we have $q_{\text{out}} \approx q_{\text{in}}$. If q_{in} grows bigger than the bottleneck capacity $q_{\text{cap}}^{\text{down}}$, the bottleneck would be activated in absence of control as in Fig. 1, and q_{out} would be reduced due to CD; while MTFC can implement a controlled mainstream flow q_{c} such that q_{out} is equal to the bottleneck capacity. Clearly, the mainstream congestion cannot be avoided via MTFC because $q_{\text{in}} > q_{\text{cap}}^{\text{down}}$, but the congestion outflow in the MTFC case is higher than in the no-control case because the CD is avoided. We use VSL as an MTFC actuator to impose the controlled flow q_{c} on the freeway mainstream.

2.2 *METANET and AMOC Tools*

A validated macroscopic second-order traffic flow model included in the METANET freeway traffic flow simulator (Messmer and Papageorgiou, 1990; Carlson et al., 2010a) is used in this work. In METANET the freeway network is represented by a directed graph, whereby the links of the graph represent freeway stretches with uniform characteristics. The nodes of the graph are placed at locations where a major change in road geometry occurs, as well as at junctions and on-/off-ramps. Adequate variables express the aggregate behavior of traffic at certain times and locations, while the time and space arguments are discretized.

The freeway network traffic control problem may be formulated as a discrete-time nonlinear dynamic optimal control problem with constrained control variables over a given optimization horizon, and is incorporated in the open-loop optimal control tool AMOC (Kotsialos et al., 2002). The cost criterion is the total time spent (TTS) by all vehicles in the network; penalty terms are added to penalize abrupt time variations of VSL and RM rates. The solution determined by AMOC consists of the optimal VSL and RM rate trajectories and the corresponding optimal state trajectory.

2.3 *VSL as an MTFC Actuator*

The reasons and ways of using VSL as an MTFC actuator have been discussed by Carlson et al. (2010a, 2010b, 2011). In short, lower VSL values induce lower capacity values. This implies that, if the mainstream demand q_{in} (Fig. 2) is higher than the VSL-induced capacity, then the VSL application area may become an active mainstream

Fig. 2. A local aspect of MTFC.

bottleneck that limits the area's outflow q_{c} to values corresponding to the (lower) VSL-induced capacity. Thus, a controllable mainstream congestion may be created upstream of a bottleneck location to avoid its activation and the related reduction of throughput because of the CD. Additionally, lower VSL values shift the critical density of the fundamental diagram, at which flow is at capacity, toward higher values.

2.4 *Practical VSL Application Aspects*

This section summarizes some practical VSL implementation aspects detailed by Carlson et al. (2011). VSL can only take discrete values via a set of admissible discrete VSL rates $b \in \{0.2, 0.3, \ldots, 1.0\}$, where a VSL rate is defined as the displayed VSL divided by the legal speed limit without VSL. The VSL to be applied is obtained by rounding-off the VSL rate b delivered by the MTFC strategy (see Section 3.2) to the nearest discrete value. Additional VSL may be activated within and upstream of the controlled congestion in a way that leads to equal VSL displays along the congested stretch; while vehicles driving towards the congestion tail encounter gradually decreasing VSL. Furthermore, the difference between two consecutive posted VSL rates at the same gantry is limited to 0.2, while the same limit applies to the difference between the posted VSL rates at two consecutive gantries. Finally, a constant VSL rate of 0.9 is applied in the acceleration and bottleneck areas whenever the MTFC via VSL is active. These practical aspects are only considered when applying feedback concepts, not with AMOC.

3. FREEWAY TRAFFIC FEEDBACK CONTROL

3.1 *PI-ALINEA*

PI-ALINEA (Wang and Papageorgiou, 2006) is a feedback RM strategy corresponding to a proportional-integral (PI) controller structure. PI-ALINEA orders suitable on-ramp inflows to the freeway based on the bottleneck density ρ_{out} (veh/km/lane), and reads:

$$\bar{q}_{\text{r}}(k) = \bar{q}_{\text{r}}(k-1) + \left(\bar{K}_{\text{P}} + \bar{K}_{\text{I}}\right) e_{\rho}(k) - \bar{K}_{\text{P}} e_{\rho}(k-1) \qquad (1)$$

where $\bar{q}_{\text{r}}$ (veh/h) is the ordered ramp flow, bounded within $\bar{q}_{\text{r}} \in \left[q_{\text{r,min}}, q_{\text{r,max}}\right]$, $\bar{K}_{\text{I}}$ and $\bar{K}_{\text{P}}$ are the integral and proportional gains, respectively, and $e_{\rho}(k) = \hat{\rho}_{out} - \rho_{out}(k)$ is the density control error with $\hat{\rho}_{out}$, the set-point, usually set around the critical density ρ_{cr} at which q_{out} is maximised.

When the on-ramp storage space is limited, queue management (QM) operates in conjunction with RM to avoid over-long ramp queues. A proportional (P) controller with

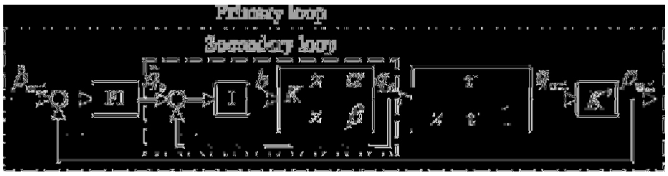

Fig. 3. Feedback cascade MTFC controller structure using VSL as actuator.

feed-forwarded on-ramp demand d (veh/h) may be used (Smaragdis and Papageorgiou, 2003):

$$\hat{q}_{\mathrm{r}}(k) = -\frac{1}{T_{\mathrm{c}}}\left[\hat{w} - w(k-1)\right] + d(k-1) \tag{2}$$

where $\hat{q}_{\mathrm{r}} \in \left[0, q_{\mathrm{r,max}}\right]$ is the queue-management ordered inflow, T_{c} (h) is the control period, w (veh) is the on-ramp queue length, and $\hat{w}$ (veh) is the maximum admissible on-ramp queue (set-point). The final ordered on-ramp inflow to the freeway is $q_{\mathrm{r}} = \max\{\bar{q}_{\mathrm{r}}, \hat{q}_{\mathrm{r}}\}$.

3.2 Feedback MTFC via VSL

The control problem here is to regulate the traffic density ρ_{out} (Fig. 2) via real-time changes of the mainstream flow q_{c} enabled by VSL (Carlson et al., 2011). Thus, we have the VSL rate b as the control input and the bottleneck density ρ_{out} as the control output.

Fig. 3 depicts the MTFC feedback cascade controller designed by Carlson et al. (2011) with α, β, $\tau > 0$, $K' > 0$, and $K > 0$ being model parameters, where $0 < \beta < \alpha \le 1$; z the discrete-time complex variable. The secondary loop in is affected by the VSL rate b delivered by the secondary controller that will determine the outflow q_{c} of Fig. 2. This flow is measured downstream of the VSL application area and is fed back and compared to the reference flow $\hat{q}_{\mathrm{c}}$ delivered by the primary controller. The primary loop uses the measured density ρ_{out} at the bottleneck area.

The secondary controller of Fig. 3 was designed as an integral (I) controller:

$$b(k) = b(k-1) + K_{\mathrm{I}} e_{\mathrm{q}}(k), \tag{3}$$

with K_{I} the integral gain and $e_{\mathrm{q}}(k) = \hat{q}_{\mathrm{c}}(k) - q_{\mathrm{c}}(k)$ the flow control error, given per lane. The primary controller was specified to be a PI controller:

$$\hat{q}_{\mathrm{c}}(k) = \hat{q}_{\mathrm{c}}(k-1) + \left(K'_{\mathrm{P}} + K'_{\mathrm{I}}\right) e_{\mathrm{p}}(k) - K'_{\mathrm{P}} e_{\mathrm{p}}(k-1) \tag{4}$$

where K'_{I} and K'_{P} are the integral and proportional gains, respectively. Similarly to RM, the density set-point $\hat{\rho}_{\mathrm{out}}$ may be set equal to the critical density ρ_{cr} for maximum throughput. For more details about the controller design, tuning and operation, see (Carlson et al., 2011).

3.3 Integrated Traffic Control

The idea in the integrated case is to specify combined mainstream and on-ramp flow values in order to keep the bottleneck density ρ_{out} around the critical density (set-point).

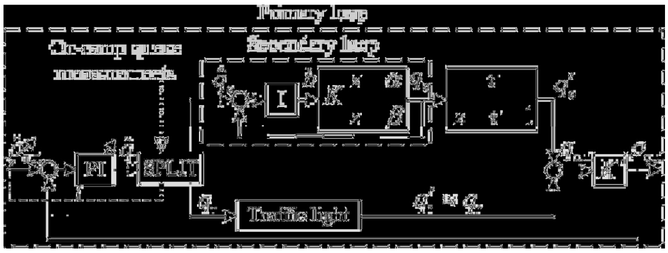

Fig. 4. Integrated feedback controller structure.

Since there are now two input flows to control the bottleneck density, there is an additional degree of freedom that may be used to apply some desired policy. The policy pursued in this paper is to apply RM for as long as the ramp storage space is not full; and to switch to MTFC only when QM is activated. This policy may be implemented if the feedback cascade control structure of Fig. 3 is extended via a split-range-like control scheme (Stephanopoulos, 1984), as depicted in Fig. 4.

In Fig. 4 the PI controller of the primary loop delivers a reference flow $\hat{q}_{\mathrm{t}}$, i.e., the total desired inflow into the bottleneck. Then, $\hat{q}_{\mathrm{t}}$ is split into the desired mainstream flow $\hat{q}_{\mathrm{c}}$, which is handled by the respective secondary loop (as in Fig. 3), and the desired RM flow q_{r} which is directly implemented via a metering policy of the traffic lights (Papageorgiou and Papamichail, 2008) to produce the respective outflows q'_{c} and q'_{r} that enter the bottleneck area.

In the split block, any change of $\hat{q}_{\mathrm{t}}$ ordered by the primary controller is conveyed to q_{r}, unless one of two restrictions apply: i) the lower RM bound $q_{\mathrm{r,min}}$ has been reached, or ii) the QM orders a higher value, in which case the final RM ordered flow q_{r} is set equal to $\hat{q}_{\mathrm{r}}$. More precisely, if $q_{\mathrm{cap}}^{\mathrm{m}}$ is the mainstream capacity and $q_{\mathrm{cap}}^{\mathrm{r}}$ is the on-ramp capacity, we have $\hat{q}_{\mathrm{t}} \le q_{\mathrm{cap}}^{\mathrm{m}} + q_{\mathrm{cap}}^{\mathrm{r}}$ by definition, and

$$q_{\mathrm{r}} = \begin{cases} \hat{q}_{\mathrm{t}} - q_{\mathrm{cap}}^{\mathrm{m}} & \text{if} \quad \hat{q}_{\mathrm{t}} - q_{\mathrm{cap}}^{\mathrm{m}} \ge \max\left(q_{\mathrm{r,min}}, \hat{q}_{\mathrm{r}}\right) \\ \max\left(q_{\mathrm{r,min}}, \hat{q}_{\mathrm{r}}\right) & \text{else} \end{cases} \tag{5}$$

$$\hat{q}_{\mathrm{c}} = \begin{cases} q_{\mathrm{cap}}^{\mathrm{m}} & \text{if} \quad \hat{q}_{\mathrm{t}} - q_{\mathrm{cap}}^{\mathrm{m}} \ge \max\left(q_{\mathrm{r,min}}, \hat{q}_{\mathrm{r}}\right) \\ \hat{q}_{\mathrm{t}} - \max\left(q_{\mathrm{r,min}}, \hat{q}_{\mathrm{r}}\right) & \text{else} \end{cases} \tag{6}$$

In essence, the controller operates as PI-ALINEA until one of the two restrictions applies, at which point it starts operating as MTFC via VSL, and the term $\max\left(q_{\mathrm{r,min}}, \hat{q}_{\mathrm{r}}\right)$ becomes a feed-forward element affecting the output of the primary controller. The gains of the primary controller should be scheduled based on the split decision, i.e., PI-ALINEA gains are used if the first condition in (5) and (6) applies, otherwise MTFC gains are used. Similarly, the set-point $\hat{\rho}_{\mathrm{out}}$ of the primary controller must be changed accordingly, since the VSL value applied at the acceleration and bottleneck areas in the MTFC case shifts the critical density to higher values.

4. SIMULATION RESULTS

The simulated scenarios are summarized in Table 1. The detailed results of optimal control are omitted, except for the integrated control case. Nevertheless, the resulting TTS for all optimal control scenarios are provided in Table 1 as a reference of achievable performance. The model parameters

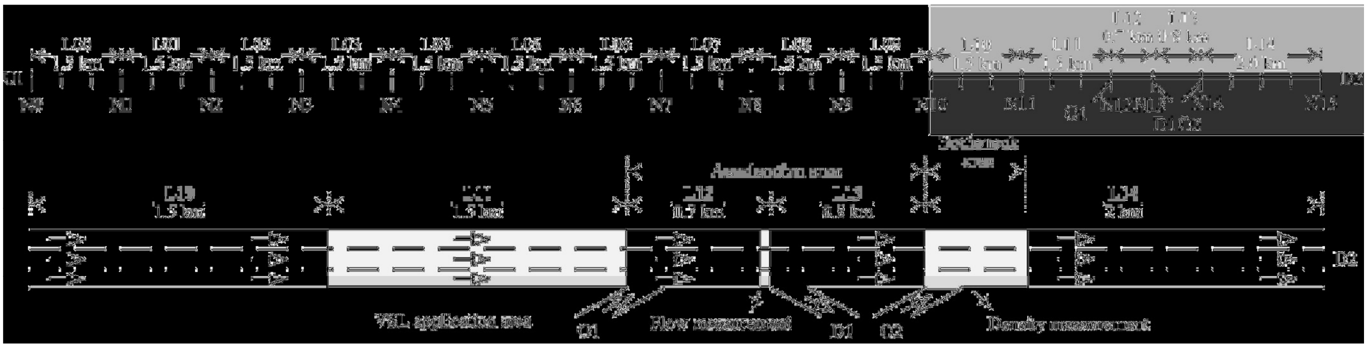

Fig. 5. Hypothetical freeway stretch.

Table 1. Summary of simulated control scenarios

Control strategy	Description	TTS	%
No control	-	4196	-
RM-AMOC	Optimal RM without ramp queue constraint.	3279	-21.9
RM-AMOC/Q	Optimal RM with maximum ramp queue of 100 veh.	3506	-16.4
PI-ALINEA	Feedback RM without ramp queue constraint.	3282	-21.8
PI-ALINEA/Q	Feedback RM with maximum ramp queue of 100 veh.	3506	-16.4
MTFC-AMOC	Optimal MTFC via VSL.	3363	-19.8
MTFC-FB	Feedback MTFC via VSL.	3370	-19.7
Integrated-AMOC	Optimal integrated control, i.e., constrained RM and MTFC via VSL.	3335	-20.5
Integrated-FB	Feedback integrated control, i.e., constrained RM and MTFC via VSL	3324	-20.8

were taken from (Carlson et al., 2010a).

4.1 Network and Demand

A hypothetical 21.5 km long three-lane freeway stretch, sketched in Fig. 5 (upper part), is used in the simulations that follow. The mainstream is divided in 15 links (L00-L14) with two on-ramps (O1 and O2) and one off-ramp (D1). The VSL application area, acceleration area, bottleneck area, and the real-time measurements for feedback control, are indicated in Fig. 5 (lower part). Depending on the control scenario, only the mainstream flow is controlled (MTFC via VSL), or only the O2 on-ramp flow (RM), or both (Integrated Control). The O1 on-ramp is left uncontrolled in all scenarios.

The demand profiles and exit rates displayed in Fig. 6 are used. The model time step is $T = 10$ s. The minimum admissible VSL rate is $b_{\min} = 0.2$ and the minimum admissible RM rate is $q_{\mathrm{r,min}} = 200$ veh/h. The control period, that determines the frequency of posted VSL changes and RM rate updates, is chosen as $T_{\mathrm{c}} = 60$ s, see (Wang and Papageorgiou, 2006; Carlson et al., 2011).

4.2 No Control

In absence of control, the resulting ramp queue, density and flow at the bottleneck area are shown in Fig. 7. The flow in the bottleneck area reaches the factual capacity (6240 veh/h) at $t = 0.4$ h, and a congestion appears there at $t = 0.5$ h; this leads to a gradual mainstream flow decrease (capacity drop).

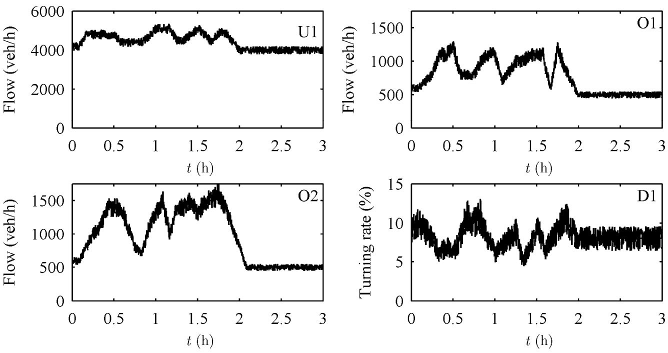

Fig. 6. Demand at the origins and turning rates.

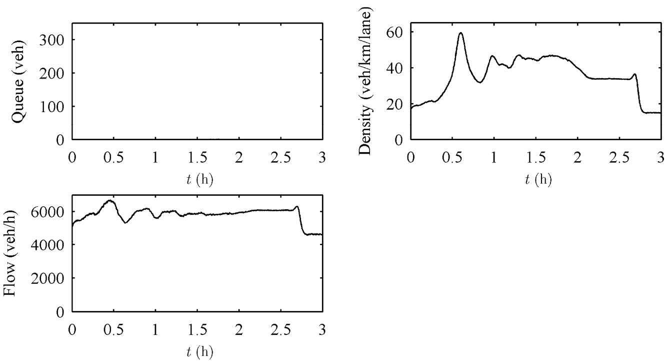

Fig. 7. No-control: ramp queue, density and flow at the bottleneck area.

The congestion travels upstream (not shown) and covers the D1 exit. Despite the lower demand entering the network after $t = 2$ h, it takes about 40 minutes before congestion is completely dissolved. The resulting TTS is 4,196 veh·h.

4.3 Ramp Metering

For the application of RM, two cases are considered in order to highlight the effect of limited on-ramp storage space. In the first case the on-ramp's storage capacity is unlimited. In the second case, the storage space is limited to 100 veh. The PI-ALINEA gains are $\bar{K}_{\mathrm{I}} = 120$ km/h/lane and $\bar{K}_{\mathrm{P}} = 300$ km/h/lane, and the set-point is $\hat{\rho}_{\mathrm{out}} = 29$ veh/km/lane.

1) Unlimited on-ramp storage space: The resulting TTS for PI-ALINEA is 3,282 veh·h, which is a 21.8 % improvement compared to the no-control case. The ramp queue, density and flow at the bottleneck area are shown in Fig. 8.

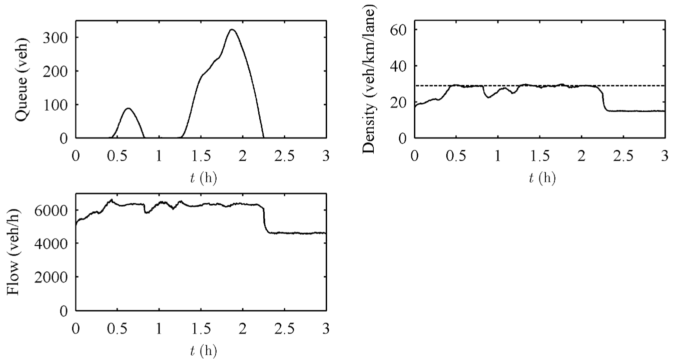

Fig. 8. PI-ALINEA: ramp queue, density and flow at the bottleneck area.

The situation is identical to the no-control case until short before $t = 0.4$ h, when the feedback controller is activated and maintains the bottleneck density close to the set-point (dashed line in the density plot) leading to maximum exit flow (and hence to minimization of TTS). To achieve this, a ramp queue is created at the O2 on-ramp in two occasions, and, since there are no queue constraints, the queue exceeds 300 vehicles in the second one. The congestion is completely avoided, and RM is even de-activated for about 20 minutes between the two demand peaks.

2) Limited on-ramp storage space: The resulting TTS for PI-ALINEA/Q is 3,506 veh·h, which is a 16.4 % improvement compared to the no-control case, but 5 % worse than in the PI-ALINEA case. Note that a storage space of 100 veh is relatively large, and was chosen to allow for a better demonstration of the integrated control scenario. The ramp queue, density and flow at the bottleneck area are shown in Fig. 9. The dotted curve in the queue plot corresponds to $\hat{w}$.

The situation is identical to the previous scenario until short before $t = 1.4$ h, when the on-ramp storage space is about to be exceeded, and QM is activated. As a consequence, the critical density at the bottleneck cannot be sustained anymore, in contrast with the PI-ALINEA case. Hence, congestion is formed thereafter, leading to a CD.

4.4 Mainstream Traffic Flow Control

For the application of MTFC-FB, the links from L01 to L11 are considered each as a cluster (each cluster having an independent VSL), and another cluster comprises links L12, L13 and L14. VSL is not applied at link L00. Link L11 is the application area where the VSL rate delivered by the control law (3) is applied after any constraints are imposed. The VSL rates at the other links follow the rules outlined in Section 2.4. The measurements are taken as shown in Fig. 5. The set-point of the primary controller is $\hat{\rho}_{\text{out}} = 32$ veh/km/lane. The controller gains are $K_{\text{I}} = 0.0007$ h/veh/lane for the secondary controller and $K'_{\text{I}} = 3$ km/h/lane and $K'_{\text{P}} = 50$ km/h/lane for the primary controller (Carlson et al., 2011).

The resulting TTS is 3,370 veh·h, which is a 19.7 % improvement compared to the no-control case. The ramp queue, density and flow at the bottleneck area, and the VSL rates are shown in Fig. 10. The situation is identical to the no-

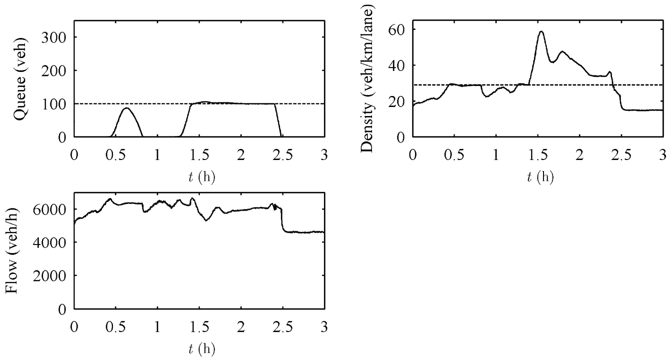

Fig. 9. PI-ALINEA/Q: ramp queue, density and flow at the bottleneck area.

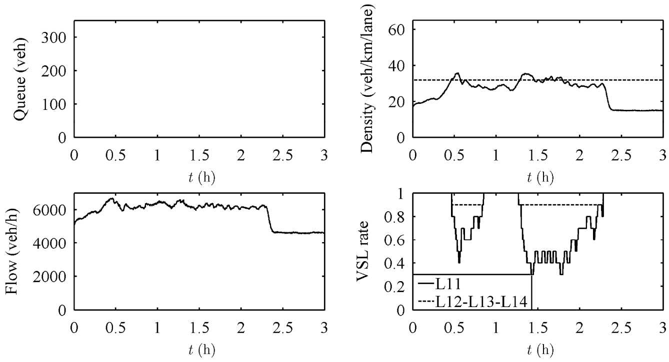

Fig. 10. MTFC-FB: ramp queue, density and flow at the bottleneck area, and the VSL rates.

control case until $t = 0.4$ h, when VSL is first activated at both clusters of links so as to decrease the flow arriving at the bottleneck and increase the critical density in the bottleneck merge area, respectively. This short VSL action is sufficient to avoid the onset of congestion, and thus further VSL action is not needed for the next 20 minutes, similarly to the PI-ALINEA case. A second, more durable control action is started short before $t = 1.3$ h holding back traffic on the mainstream. The bottleneck congestion is again avoided and the outflow is maintained close to capacity by maintaining the bottleneck density close to its set-point $\hat{\rho}_{\text{out}}$ (dashed line in the density plot). Note that the resulting improvement is slightly lower than in the RM case with unlimited storage; this is because MTFC restricts the mainstream flow upstream of the off-ramp, and hence the off-ramp outflow is reduced accordingly; thus, some delays are incurred for the vehicles bound for the off-ramp (which are avoided with RM).

4.5 Integrated Control

For the application of Integrated-AMOC, only link L11 and the cluster comprising links L12, L13 and L14 are controlled. The on-ramp queue is limited to 100 veh. The resulting TTS is 3,335 veh·h, which is a 20.5 % improvement compared to the no-control case and superior to the constrained RM cases and to the MTFC cases. The ramp queue, density and flow at the bottleneck area, and the VSL rates are shown in Fig. 12.

Up to around $t = 1.4$ h, there is no significant difference from the two RM scenarios investigated previously. AMOC

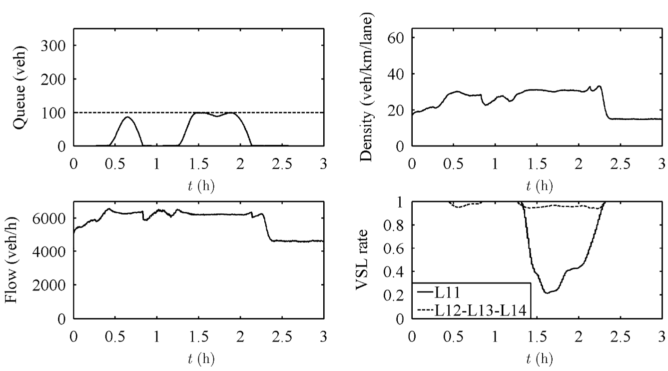

Fig. 12. Integrated-AMOC: ramp queue, density and flow at the bottleneck area, and the VSL rates.

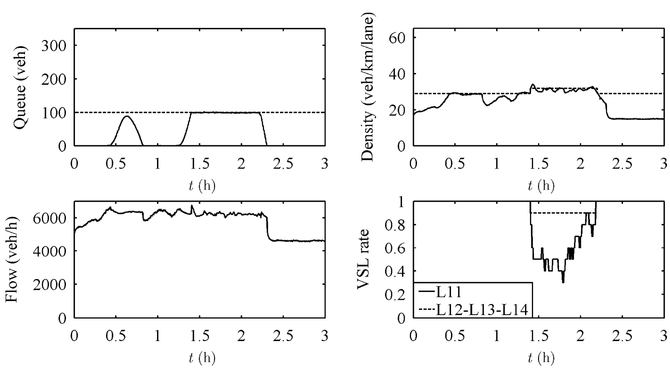

Fig. 11. Integrated-FB: ramp queue, density and flow at the bottleneck area, and the VSL rates.

has a clear "preference" for RM over MTFC in the first peak period where only RM is applied and is sufficient to avoid the congestion. In the second peak period, AMOC starts applying both control measures quasi simultaneously. AMOC efficiently keeps the on-ramp queue within the stipulated limit. Congestion is completely avoided in both peak periods.

When Integrated-FB is used, the resulting TTS is 3,324 veh·h, which is a 20.8 % improvement compared to the no-control case and in fact slightly better than in the corresponding optimal control case. The latter is because, for this specific scenario, the activation of VSL upstream of the application area affects favorably the performance of the system. The ramp queue, density and flow at the bottleneck area, and the VSL rates are shown in Fig. 11. The controller gains and set-point are the same as in Sections 4.3 and 4.4.

The results in Fig. 11 are quite similar to the corresponding optimal control scenario of Fig. 12. It is visible in the VSL rates plot of Fig. 11 that the constraints of the VSL rate, as outlined in Section 2.4, apply.

5. CONCLUSIONS

Ramp Metering (RM) and Mainstream Traffic Flow Control (MTFC) via Variable Speed Limits were integrated for the efficient control of freeway traffic. An existing cascade feedback MTFC controller was extended by use of a split-range-like scheme so as to allow integration with RM. The split control is designed in such a way that MTFC enters in operation only when the on-ramp queue is about to be exhausted. The integrated feedback control strategy remains simple and yet efficient and is deemed suitable for field application. Ongoing research is investigating the integration of RM and MTFC at the network level. A field test of the proposed strategy will be attempted in the near future.

REFERENCES

Carlson, R.C., Papamichail, I., Papageorgiou, M., (2011). Local feedback-based mainstream traffic flow control on motorways using variable speed limits. IEEE Trans. on Intelligent Transportation Systems 12, 1261–1276.

Carlson, R.C., Papamichail, I., Papageorgiou, M., Messmer, A., (2010a). Optimal motorway traffic flow control involving variable speed limits and ramp metering. Transportation Science 44, 238–253.

Carlson, R.C., Papamichail, I., Papageorgiou, M., Messmer, A., (2010b). Optimal mainstream traffic flow control of large-scale motorway networks. Transportation Research Part C 18, 193–212.

Hegyi, A., De Schutter, B., Hellendoorn, H., (2005). Model predictive control for optimal coordination of ramp metering and variable speed limits. Transportation Research Part C 13, 185–209.

Karimi, A., Hegyi, A., De Schutter, B., Hellendoorn, J., Middelham, F., (2004). Integrated model predictive control of dynamic route guidance information systems and ramp metering. In: The 7th International IEEE Conference on Intelligent Transportation Systems, Washington, D.C., USA, pp. 491–496.

Kotsialos, A., Papageorgiou, M., Mangeas, M., Haj-Salem, H., (2002). Coordinated and integrated control of motorway networks via non-linear optimal control. Transportation Research Part C 10, 65–84.

Messmer, A., Papageorgiou, M., (1990). METANET: a macroscopic simulation program for motorway networks. Traffic Engineering and Control 31, 466–470.

Papageorgiou, M., Kotsialos, A., (2002). Freeway ramp metering: an overview. IEEE Trans. on Intelligent Transportation Systems 3, 271–281.

Papageorgiou, M., Papamichail, I., (2008). Overview of traffic signal operation policies for ramp metering. Transportation Research Record 2047, 28–36.

Papamichail, I., Kotsialos, A., Margonis, I., Papageorgiou, M., (2010). Coordinated ramp metering for freeway networks – a model-predictive hierarchical control approach. Transportation Research Part C 18, 311–331.

Smaragdis, E., Papageorgiou, M., (2003). Series of new local ramp metering strategies. Transportation Research Record 1856, 74–86.

Stephanopoulos, G., (1984). Chemical process control: an introduction to theory and practice. Prentice-Hall, Englewood Cliffs N.J.

Wang, Y., Papageorgiou, M., (2006). Local ramp metering in the case of distant downstream bottlenecks. In: The 2006 IEEE Intelligent Transportation Systems Conference, Toronto, ON, Canada, pp. 426–431.

Zhang, J., Chang, H., Ioannou, P.A., (2006). A simple roadway control system for freeway traffic. In: The 2006 American Control Conference, Minneapolis, MN, USA, pp. 4900–4905.